Comparative analysis of the Mossbauer spectra of $YBa_2(Cu_{0.99}Fe_{0.01})O_{7-\ delta}$ with static distribution and relaxation models

1992 J. Phys.: Condens. Matter 4 3551

(http://iopscience.iop.org/0953-8984/4/13/017)

J. Phys.: Condens. Matter 4 (1992) 3551–3558. Printed in the UK

Comparative analysis of the Mössbauer spectra of $YBa_2(Cu_{0.99}Fe_{0.01})_3O_{7-\delta}$ with static distribution and relaxation models

Q A Pankhurst, S Suharan and M F Thomas
Department of Physics, University of Liverpool, Liverpool L69 3BX, UK

Received 30 September 1991

Abstract. The low-temperature ^{57}Fe Mössbauer spectra of superconducting samples of Fe-substituted $YBa_2Cu_3O_{7-\delta}$ containing less than ~5 at.% Fe are characterized by a broad magnetically split profile. Although there is consensus in the literature as to the shape of this spectrum, there is no consensus of interpretation. Comparison of the fits obtained for two samples with 1% Fe substitution using (i) a hyperfine-field distribution model and (ii) a dynamic relaxation model demonstrates that the distribution model is marginally better, but that the relaxation model cannot be reliably discounted on the basis of the low-temperature Mössbauer data alone.

1. Introduction

Although it is well established that at low temperatures superconducting samples of Fe-substituted $YBa_2Cu_3O_{7-\delta}$ exhibit some form of magnetic order, there is continuing debate as to the exact nature of the ordered state. Below temperatures ranging from ~15 K in 5% Fe-doped YBCO to ~3 K in 1% doped YBCO, a broad, magnetically split ^{57}Fe Mössbauer spectrum is observed. The spectrum is largely featureless, and lends itself to many possible interpretations. Examples of the most commonly proposed models are (i) an ordered magnetic system with a distribution of hyperfine fields, (ii) a collection of slowly relaxing paramagnetic Fe ions, (iii) an ordered system close to a critical temperature, undergoing slow fluctuations in magnetization, and (iv) a spin glass in which static Fe moments are frozen into random orientations with respect to each other. In terms of the procedure for fitting the Mössbauer spectrum itself, models (i) and (iv) call for a distribution of static hyperfine fields, while models (ii) and (iii) require a stochastic relaxation approach.

Many experiments have been performed by many groups in attempts at distinguishing which of the static or relaxing models is correct. It has been found that as the level of Fe doping increases, magnetic hyperfine spectra appear at progressively higher temperatures [1–3]. This can be interpreted as evidence for the static state, since in a model based on slow paramagnetic relaxation the maximum effect would occur for the largest isolation of the magnetic ions [3]. Further evidence for the static state is the observation that no significant changes occur on cooling to very low temperatures, such as 100 mK [4], ruling out the possibility that critical fluctuations are present. Neutron diffraction results have been recorded for samples containing between 5 and 15 at.% Fe that imply that there is an absence of long-range order

0953-8984/92/133551+08$04.50

in the moment directions [5]. It therefore seems that the magnetic state of the Fe ions in $YBa_2(Cu_{1-x}Fe_x)_3O_{7-\delta}$ may be that of a spin glass. Given this possibility, it is of interest to return to the low-temperature Mössbauer spectra and determine the extent to which the data provide a definitive test of the models.

Consequently, the objective of this work is to determine whether or not it is possible to distinguish between a static distribution model and a dynamic relaxation model on the basis of the low-temperature Mössbauer spectra alone. In the course of pursuing this objective, new modelling procedures have been developed, particularly for the static distribution model. These will be discussed in some detail in order that the methodology might be explicitly stated.

2. Experimental details

Two samples were prepared from a stoichiometric mix of Y_2O_3, $BaCO_3$, CuO and $^{57}Fe_2O_3$ which was repeatedly ground and heated to 950 °C in air. Sample 1 was slowly cooled (over ~24 h) from 950 °C to room temperture in air, while sample 2 was thermally quenched (in ~5 min) in an Ar atmosphere. X-ray patterns established that the samples were single phased. Oxygen contents were assessed using an oxidation titration method [6], and found to be 6.82 per formula unit for the slow cooled sample, and 6.54 for the quenched sample. Resistivity and AC susceptibility measurements showed a sharp transition to the superconducting state at T_c ~90 K for sample 1, and a broad transition leading to superconductivity at ~40 K for sample 2. These results have been described in more detail elsewhere [3].

^{57}Fe Mössbauer spectra were recorded at 1.3 K with the samples immersed in a pumped liquid helium cryostat, and at 77 K with the samples in a liquid nitrogen bath. A high-activity γ-ray source, ^{57}CoRh with ~100 mCi initial activation, was modulated using a triangular velocity waveform, and the transmitted γ-ray counts were collected into a 576-channel spectrometer. The spectra were subsequently folded to eliminate baseline curvature. Calibration was with respect to α-Fe at room temperature. The 1.3 K spectra of both samples are shown in figures 1 and 3.

3. Static distribution model

The solid curves in figure 1 correspond to the fits obtained using a static distribution model. The fitted probability distributions of hyperfine fields, $P(B_{hf})$, are shown in figure 2. The fitting algorithm that was used incorporated both linear and non-linear least-squares procedures, and was loosely based on the methods of Le Caer and Dubois [7] and Hesse and Rübartsch [8].

The fitting procedure is designed to separate the minimization of the linearly varying parameters from the more complicated routines needed for the non-linear parameters. The quantity to be minimized is the chi-squared merit function

$$\chi^2 = \sum_{i=1,\ N} \left(A \pm B(1 - X_i^2/X_0^2) - \sum_{j=1,\ M} D_j c_{ij} - y_i \right)^2 / y_i^{1/2} \qquad (1)$$

where N is the number of channels in the spectrum, y_i is the number of counts in the ith channel (i.e. the data), X_i is the source velocity in the ith channel, and X_0 is

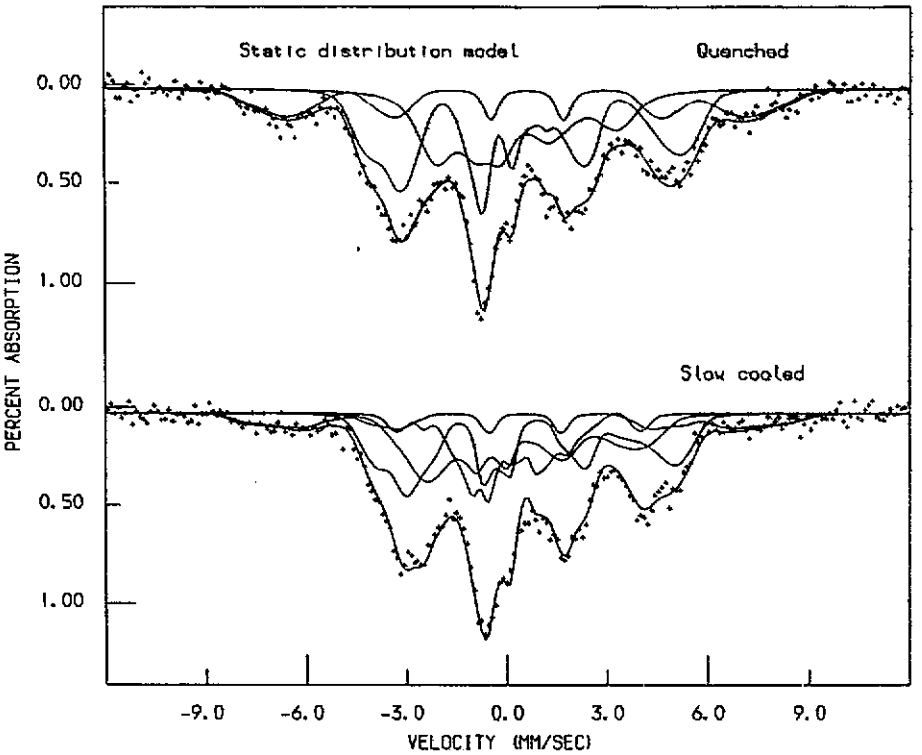

Figure 1. ^{57}Fe Mössbauer spectra at 1.3 K of a 'quenched' sample of 1% Fe-doped YBCO with composition $YBa_2(Cu_{0.99}Fe_{0.01})_3O_{6.54}$, and a 'slow-cooled' sample of composition $YBa_2(Cu_{0.99}Fe_{0.01})_3O_{6.82}$. The solid curves are the result of a least-squares fit of the data using a distribution of hyperfine-field model.

the maximum source velocity. A and B are the baseline curvature coefficients of the unfolded spectrum, and the $\pm$ sign accounts for the different signs of curvature on each half of the spectrum. The term $\sum_{j=1,\ M} D_j c_{ij}$ represents the calculated spectrum in channel i, where D_j is the area of the jth subcomponent spectrum c_{ij} and M is the number of subcomponent spectra.

The computed subspectra c_{ij} depend non-linearly on the implicitly defined hyperfine parameters, but the parameters A, B and D_j are linear since the equations

$$\partial\chi^2/\partial A = 0 \qquad \partial\chi^2/\partial B = 0 \qquad \partial\chi^2/\partial D_j = 0 \qquad \text{where } j = 1, \ldots, M \quad (2)$$

provide a set of $M + 2$ linear algebraic equations in $M + 2$ unknowns. It is therefore a simple matter, given a set of computed c_{ij} to construct the matrix inversion problem of order $M + 2$, and to determine directly the optimum values of A, B and D_j.

In the case where the subcomponent spectra differ only by an incremental step in the value of the hyperfine field, the area parameters D_j correspond directly to the probability distribution $P(B_{hf})$. Since it is physically unrealistic that there be negative probabilities in the distribution, it is desirable to include smoothing and boundary conditions. This may be achieved by adding extra terms to the merit

function, so

$$\psi^2 = \chi^2 + \alpha \sum_{j=2,\ M-1} (D_{j-1} - 2D_j + D_{j+1})^2 + \beta \sum_k D_k^2 \qquad (3)$$

becomes the function to be linearly minimized. Here α is a smoothing coefficient and β is a boundary coefficient which favours $D_k = 0$ at any number of specified values of k.

Applying the above methodology to the problem of the Mössbauer spectra of $YBa_2(Cu_{0.99}Fe_{0.01})_3O_{7-\delta}$ is complicated by the number of distinct Fe sites that occur in the material. In oxygen-poor Fe-doped YBCO samples there are three distinct Fe sites, and in oxygen-rich samples there are four sites. These sites are characterized by their isomer shift δ, quadrupole splitting Δ, electric field gradient (EFG) asymmetry η, and the angle θ between the principal axis of the EFG and the crystallographic c axis [3, 9]. Values of δ and Δ, obtained from the fit to the 1.3 K spectra, as well as the known values of η and θ, are given in table 1.

Table 1. Isomer shift δ (in mm s^{-1}), quadrupole splitting Δ (in mm s^{-1}), mean hyperfine field $\langle B_{hf} \rangle$ (in T), asymmetry η and angle θ (in deg) between the EFG principal axis and the crystallographic c axis for the distinct Fe sites present in $YBa_2(Cu_{0.99}Fe_{0.01})_3O_{7-\delta}$. The parameters δ, Δ and $\langle B_{hf} \rangle$ were determined from a least-squares fit of the 1.3 K spectra using a $P(B_{hf})$ distribution model, while η and θ were constrained to the values indicated.

	Quenched sample					Slow-cooled sample				
Site	δ	Δ	$\langle B_{hf} \rangle$	η	θ	δ	Δ	$\langle B_{hf} \rangle$	η	θ
A	0.13	−2.02	22.0	0	0	0.12	−2.03	23.3	0	0
B	0.03	1.04	13.4	1	90	0.06	0.99	17.4	1	90
C	0.43	0.72	43.1	0	0	0.38	0.55	42.7	0	0
D						−0.02	−0.54	9.0	0	0

The multiple sites were incorporated into the $\sum_{j=1,\ M} D_j c_{ij}$ term of equation (1) by subdividing the summation range: for example, in fitting the spectrum of the oxygen-poor (quenched) sample, M was set at 100, with the subspectra c_{ij} corresponding to site A being called for $j = 1, \ldots, 40$, subspectra for site B called for $j = 41, \ldots, 80$, and subspectra for site C called for $j = 81, \ldots, 100$. Boundary conditions were imposed to ensure that the calculated values of D_k were close to zero for $k = 1, 40, 41, 80, 81$ and 100. The lack of a constraint on the overall relative areas of the A, B and C components was overcome by simultaneously fitting the 1.3 K spectrum with a 77 K paramagnetic spectrum in which the three sites were easily distinguishable as three doublets. Proper consideration was given to the temperature dependence of the isomer shift parameter.

The resultant fits were of high quality for both the quenched and slow-cooled samples (see figure 1). The mean hyperfine field at each site is given in table 1, and the full $P(B_{hf})$ curves are shown in figure 2. It is apparent that at some of the Fe sites the $P(B_{hf})$ curves are bi-modal. It is not clear whether this is a significant effect, or an artefact of the fitting caused by an overlap of the outer lines of component sextets with small fields B_{hf} and the second and fifth lines of component sextets with large fields B_{hf}. The latter is a problem that is often encountered in $P(B_{hf})$ fits. It

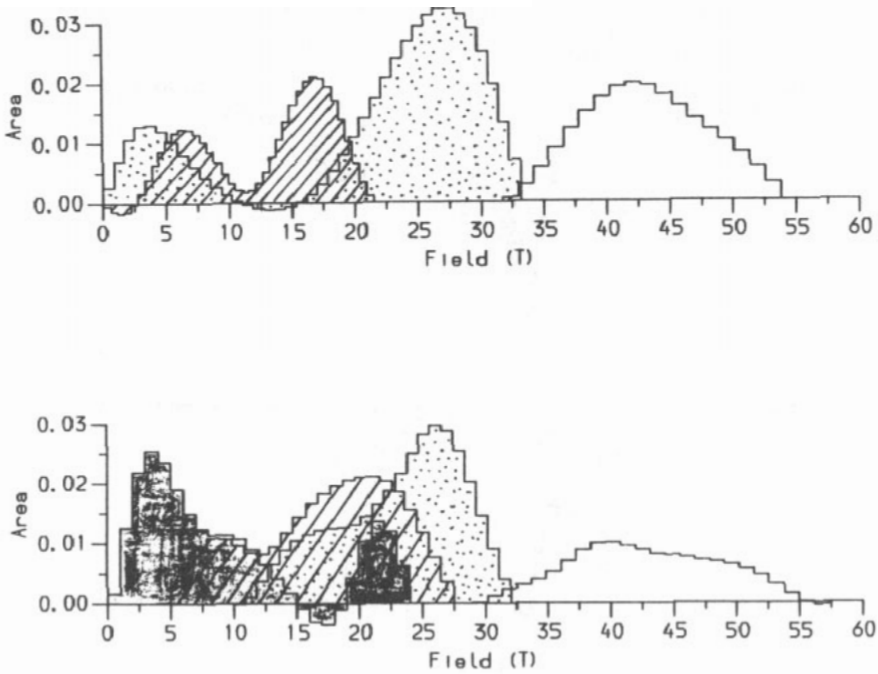

Figure 2. Fitted $P(B_{hf})$ histograms for (top) the quenched and (bottom) the slow-cooled $YBa_2(Cu_{0.99}Fe_{0.01})_3O_{7-\delta}$ samples, corresponding to the curves shown in figure 1. Three Fe sites were used for the quenched sample, and four for the slow-cooled sample. The different sites are denoted by: dotted area, site A; cross-hatched area, site B; unshaded area, site C; shaded area, site D. The summed areas under the histograms are normalized to 1.

should be noted that in the analysis each component subspectrum was calculated by a full non-perturbative consideration of both the electric quadrupole and magnetic hyperfine interactions, so the problems associated with the first-order approximation methods commonly used elsewhere are not present.

4. Relaxation model

The solid curves in figure 3 correspond to the fits obtained using a relaxation model based on the stochastic relaxation theory of Blume and Tjön [10]. In this case the linear minimization procedure described in the preceding section was applied only to the baseline curvature parameters and a single total spectral area parameter.

Within the relaxation model the broadening of the Mössbauer spectral lines is attributed to the effect of the individual Fe moments physically reorienting on a timescale comparable to the measurement scale of the Mössbauer transition, $\sim 10^{-9}$ s. The magnitude of the moment that is flipping is signified by the value of the saturation hyperfine field B_{sat} at the Fe nucleus, and the rate at which the spin flips determines the degree of line broadening in the Mössbauer spectrum.

On fitting the 1.3 K $YBa_2(Cu_{0.99}Fe_{0.01})_3O_{7-\delta}$ spectra it was found that more than one relaxation rate per Fe site was required, so three different rates (equally

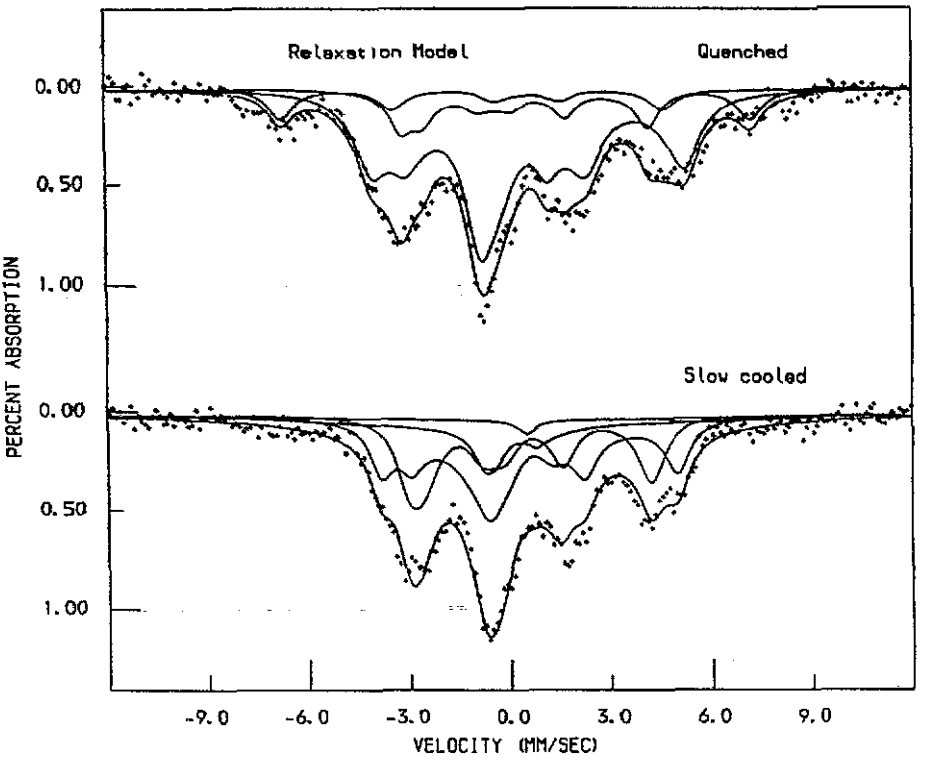

Figure 3. Mössbauer spectra, as in figure 1, fitted using a stochastic relaxation model.

weighted by spectral area) were allowed for each site. A limitation on the number of rates used was imposed by the complexity of the relaxation model itself, and the consequent heavy demand on computer resources. Once again the relative areas of the different Fe-site components were constrained by simultaneously fitting the 1.3 K and 77 K spectra.

Table 2. Isomer shift δ (in mm s^{-1}), quadrupole splitting Δ (in mm s^{-1}), saturation hyperfine field B_{sat} (in T) and mean relaxation rate $\langle Rate \rangle$ (in MHz) determined from a least-squares fit of the 1.3 K spectra using a stochastic relaxation model.

	Quenched sample				Slow-cooled sample			
Site	δ	Δ	B_{sat}	$\langle Rate \rangle$	δ	Δ	B_{sat}	$\langle Rate \rangle$
A	0.13	−2.00	27.8	243	0.12	−2.03	26.6	99
B	0.06	0.91	22.6	11	0.05	1.12	22.3	24
C	0.42	0.69	43.2	22	0.39	0.57	49.3	140
D					−0.01	−1.55	36.1	713

The resultant fits are shown in figure 3, and the fitted parameters are given in table 2. Values of η and θ were constrained to be the same as those used in the $P(B_{hf})$ model. The fitted values of δ and Δ compare favourably with those found using the $P(B_{hf})$ model, and the values of B_{sat} are all greater than the values of $\langle B_{hf} \rangle$ found using the $P(B_{hf})$ model, as is to be expected.

5. Results and conclusions

Visual inspection of the least-squares fits of the 1.3 K spectra of 1% Fe-doped $YBa_2Cu_3O_{7-\delta}$ obtained using $P(B_{hf})$ distribution and relaxation models, figures 1 and 3, reveals that both models give satisfactory results. This is confirmed by the respective values of the χ^2 merit function obtained for the fits (see table 3), which are not very different. However, close inspection of the data leads to the conclusion that the $P(B_{hf})$ distribution model is the better of the two in correctly following the features evident in the spectra. This is especially evident in the outermost lines of the spectra, and in the area of absorption near +2 mm s^{-1}. It is therefore apparent that although it would be difficult to distinguish between the validity of the $P(B_{hf})$ and relaxation models on the basis of the low-temperature spectra alone, in the light of supporting evidence from other sources it is likely that the static distribution model is the more appropriate of the two.

Table 3. The χ^2 figures of merit obtained from the computer fits of the 1.3 K Mössbauer spectra of $YBa_2(Cu_{0.99}Fe_{0.01})_3O_{7-\delta}$ using static distribution and dynamic relaxation models.

Model	Quenched sample	Slow-cooled sample
$P(B_{hf})$ distribution	χ^2 = 1.18	1.23
Relaxation	1.44	1.52

Further to this conclusion, it is interesting to enquire further about the nature of the magnetic state: is it an ordered system with a hyperfine-field distribution, or a spin glass? Neutron diffraction data imply that it is a spin glass. The $P(B_{hf})$ distribution model used in this work was in fact based on the assumption of an ordered magnetic system in which every hyperfine field at a given Fe site had the same orientation in the crystalline lattice. If the system were a spin glass, each Fe site would be occupied by a collection of randomly directed hyperfine-field vectors, with a distribution of magnitudes B_{hf} superimposed. The result would be a random sampling of the crystalline electric field gradient at each site. To model the Mössbauer spectrum resulting from such a system it would be necessary to compute each individual subspectrum in a $P(B_{hf})$ distribution as a superposition of 'sub-subspectra' corresponding to representative orientations of B_{hf} vectors in the crystalline coordinate system. This is orders of magnitude more complex than the analysis used in the present work, and would exceed our current computing resources. We conclude that at present we are unable to determine the exact nature of the low-temperature magnetic state in $YBa_2(Cu_{0.99}Fe_{0.01})_3O_{7-\delta}$ on the basis of the low-temperature Mössbauer spectra alone.

References

[1] Zhou X Z, Raudsepp M, Pankhurst Q A, Morrish A H, Luo Y L and Maartense I 1987 *Phys. Rev.* B **36** 7230

[2] Nasu S, Kitagawa H, Yoshida M, Oda Y, Ueda K, Kohara T, Shinjo T, Asayama K and Szucs I S 1990 *Hyperfine Interact.* **55** 1229

[3] Suharan S, Johnson C E, Pankhurst Q A and Thomas M F 1991 *Solid State Commun.* **78** 897

[4] Shinjo T, Nasu S, Kohara T, Takabataka T and Ishikawa M 1988 *J. Physique Coll.* **49** C8 2207
[5] Katano S, Matsumoto A, Matsushita A, Hatano T and Funahashi S 1990 *Phys. Rev.* B **41** 2009
[6] Suharan S, Jones D H, Johnson C E, Pankhurst Q A and Thomas M F 1990 *Hyperfine Interact.* **55** 1387
[7] Le Caer G and Dubois J M 1979 *J. Phys. E: Sci. Instrum.* **12** 1083
[8] Hesse J and Rübartsch A 1974 *J. Phys. E: Sci. Instrum.* **7** 168
[9] Brand R A, Sauer C, Lutgemeier H, Mueffles P M and Zinn W 1990 *Hyperfine Interact.* **55** 1229
[10] Blume M and Tjön J A 1968 *Phys. Rev.* **165** 446